

## Magnetometry using Ramsey interferometry in a Yb atomic beam

Ketan D. Rathod and Vasant Natarajan\*

Department of Physics, Indian Institute of Science,  
Bengaluru 560 012, India

We use the Ramsey separated oscillatory fields technique in a 400°C thermal beam of ytterbium (Yb) atoms to measure the Larmor precession frequency (and hence the magnetic field) with high precision. For the experiment, we use the strongly allowed  $^1S_0 \rightarrow ^1P_1$  transition at 399 nm, and choose the odd isotope  $^{171}\text{Yb}$  with nuclear spin  $I = 1/2$ , so that the ground state has only two magnetic sublevels  $m_F = \pm 1/2$ . With a magnetic field of 22.2 G and a separation of about 400 mm between the oscillatory fields, the central Ramsey fringe is at 16.64 kHz and has a width of 350 Hz. The technique can be readily adapted to a cold atomic beam, which is expected to give more than an order-of-magnitude improvement in precision. The signal-to-noise ratio is comparable to other techniques of magnetometry; therefore it should be useful for all kinds of precision measurements such as searching for a permanent electric dipole moment in atoms.

**Keywords:** Magnetometry, oscillatory fields, precession frequency, ytterbium atoms.

SENSITIVE magnetometry allows optical detection of level crossings in the shot noise limit<sup>1</sup>, and has important applications in precision measurements such as the search for a permanent electric dipole moment (EDM) in atoms<sup>2</sup>. In the absence of collisions, the linewidth of the magnetic resonance is determined by the finite interaction time of the atoms with the light field. As in conventional magnetic resonance experiments, line narrowing is achieved using Ramsey's technique of separated oscillatory fields (SOFs)<sup>3</sup>. SOF on an atomic beam can reach the same precision in magnetometry as other cell-based techniques, but has the additional advantage of being less sensitive to field variations, both spatial and temporal. For example, in another high-precision technique called nonlinear magneto-optic rotation (NMOR) – also demonstrated in our group recently<sup>4</sup> – the resonance linewidth is limited by field inhomogeneities<sup>5</sup>, but in SOF measurements the linewidth depends only on the separation between the pump and probe regions, while the average field in this region determines the location of the central fringe.

In this work, we demonstrate the use of the SOF technique for sensitive magnetometry in a thermal beam of ytterbium (Yb) atoms. We use the strongly allowed  $^1S_0 \rightarrow ^1P_1$  transition at 399 nm, and the odd isotope  $^{171}\text{Yb}$  with nuclear spin  $I = 1/2$ .  $^{171}\text{Yb}$  atoms emanating from a

thermal source are first optically pumped to the  $m_F = -1/2$  ground sublevel using a  $\sigma^-$  pump beam. The atoms then pass through two rf interaction zones in a region that has a uniform quantization magnetic field which determines the Larmor precession frequency. The rf strength and interaction length of each zone are adjusted to give a  $\pi/2$  pulse for atoms travelling with the mean velocity of 340 m/s. The two rf zones are separated by  $\sim 400$  mm. The fraction of atoms left in  $m_F = -1/2$  ground sublevel after the second interaction is measured using a  $\sigma^+$  probe beam. The fluorescence signal from the probe as the rf frequency is scanned around the Larmor frequency shows a characteristic interference fringe pattern with a central fringe located at 16.64 kHz having a linewidth of 350 Hz. Both the lineshape and linewidth agree with the calculated probability of transition averaged over the thermal velocity distribution. For EDM measurements, the signature of an EDM would be a shift in the fringe pattern correlated with the application of an electric field. The signal-to-noise ratio (SNR) is better than the rival magnetometry technique of NMOR<sup>4</sup>.

The relevant parts of the set-up are shown schematically in Figure 1. The experiments are done inside a ultrahigh vacuum (UHV) chamber. The atomic beam is generated by resistively heating a quartz ampoule containing elemental Yb to a temperature of about 400°C. The source is not enriched and contains all isotopes in their natural abundances. The source part is maintained at a pressure of  $10^{-7}$  torr by a 20 l/s ion pump. It is connected to the main experimental chamber consisting of a tube that is 500 mm long with outside diameter (OD) of 42 mm, sandwiched between ports for optical access. This part is maintained at a pressure of  $10^{-9}$  torr by a 75 l/s ion pump. There is a differential pumping tube of 5 mm inside diameter (ID)  $\times$  50 mm length between the source and the experimental chamber. It serves the dual purpose of (i) allowing a pressure differential between the two regions, and (ii) collimating the atomic beam.

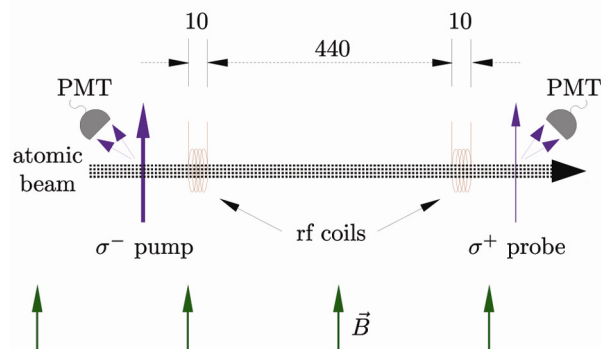


**Figure 1.** (Colour on-line). Schematic of the main parts of the experimental set-up. A pair of rectangular coils (not shown), placed on either side of the atomic beam, produces the quantization magnetic field.

\*For correspondence. (e-mail: profvasant@gmail.com)

The atomic beam emerging from the differential pumping tube passes through a region with a constant magnetic field  $B$  in the transverse direction. This field is produced by a pair of rectangular coils with dimensions 800 mm  $\times$  130 mm and separated by 160 mm, placed on the outside of the vacuum chamber. Each coil consists of six turns of 8 mm thick welding wire wound around four steel rods to provide shape and support. The coils carry a current 65 A so as to produce a field of about 22 G at the location of the atomic beam.

The required rf fields are produced using two coils wound around the outside of the 42 mm OD vacuum tube. Each coil is made using insulated copper wire of 0.6 mm diameter, and consists of 90 turns in six layers. The physical width of the rf coils is 10 mm and they are separated by 440 mm, as shown in the figure. The coils are driven with the output of a function generator amplified by a home-built audio amplifier.

The laser beams needed for the experiment are generated using a grating stabilized diode laser (Toptica DL100), operating with a Nichia diode at 399 nm. The linewidth of the laser after feedback is about 1 MHz, and the total power available is 10 mW. The laser is locked to a particular magnetic transition (as described later in the text) using current modulation at 20 kHz. The pump beam has  $1/e^2$  diameter of 2.3 mm and power 2.2 mW, and is  $\sigma^-$  polarized. It is used to spin polarize the unpolarized atoms coming out of the oven, by optically pumping into the  $m_F = -1/2$  ground sublevel. The probe beam has  $1/e^2$  diameter of 1 mm and power of 50  $\mu$ W, and is  $\sigma^+$  polarized. It is used to detect the population left in the  $m_F = -1/2$  sublevel after the second rf interaction. All signals are fluorescence type picked up with photomultiplier tubes (PMTs) from Hamamatsu (R928).

The Zeeman shift (Hz) of a sublevel with a given value of  $m_F$  is

$$\delta\nu = g_F \mu_B m_F B, \quad (1)$$

where  $g_F$  is the  $g$  factor of the level,  $\mu_B = 1.4$  MHz/G is the Bohr magneton and  $B$  is the magnetic field (G). For the hyperfine level  $F$ ,  $g_F$  is given by<sup>6</sup>

$$g_F = g_J \frac{F(F+1) + J(J+1) - I(I+1)}{2F(F+1)} - g_I \frac{\mu_N}{\mu_B} \frac{F(F+1) + I(I+1) - J(J+1)}{2F(F+1)}, \quad (2)$$

where  $J$  is the total electronic angular momentum,  $I$  the nuclear spin,  $g_J$  the Landé  $g$  factor,  $g_I$  the nuclear  $g$  factor and  $\mu_N$  is the nuclear magneton.

For the  $^1S_0$  ground state in  $^{171}\text{Yb}$ ,  $J$  is 0 and so the first term in eq. (2) is 0 and only the second term contributes. The nuclear magnetic moment<sup>7</sup>  $\mu_n$  for  $^{171}\text{Yb}$  is

+0.4926  $\mu_N$ . Using  $\mu_n = g_I \mu_N I$ , the  $g$  factor for the  $F = 1/2$  level is

$$g_F = -5.37 \times 10^{-4}.$$

From eq. (1), this gives a shift of  $-375$  Hz/G for the  $m_F = +1/2$  sublevel.

For the excited  $^1P_1$  state,  $J$  is 1 and so both terms in eq. (2) are potentially important. But we can ignore the second term since  $\mu_N/\mu_B = 1/1836$ . Thus the  $g$  factor for the  $F' = 1/2$  level is

$$g_{F'} = +1.33.$$

This gives a shift of +0.93 MHz/G for the  $m_{F'} = +1/2$  sublevel, which is opposite in sign to the ground state because of the opposite signs of the  $g$  factors. The splitting of these two levels in a magnetic field of 22 G is shown in Figure 2. The ground level splitting gives the Larmor precession frequency; so it is 16.5 kHz for this field.

Once an atom is pumped into the  $m_F = -1/2$  sublevel, there is a probability  $p$  that it has made a transition to the  $m_F = +1/2$  sublevel after interacting with the two rf fields. If the two rf zones have a length  $\ell$  and are separated by a distance  $L$ , the atom has a velocity  $v$ , and the rf field has a strength  $\Omega_R$  (its Rabi frequency), and its frequency is detuned from resonance by  $\Delta$ . The transition probability is given by<sup>3</sup>

$$p = 4 \frac{\Omega_R^2}{\Omega_R'^2} \sin^2 \left( \frac{\Omega_R' \ell}{2v} \right) \times \left[ \cos \frac{\Delta L}{2v} \cos \frac{\Omega_R' \ell}{2v} - \frac{\Delta}{\Omega_R'} \sin \frac{\Delta L}{2v} \sin \frac{\Omega_R' \ell}{2v} \right]^2, \quad (3)$$

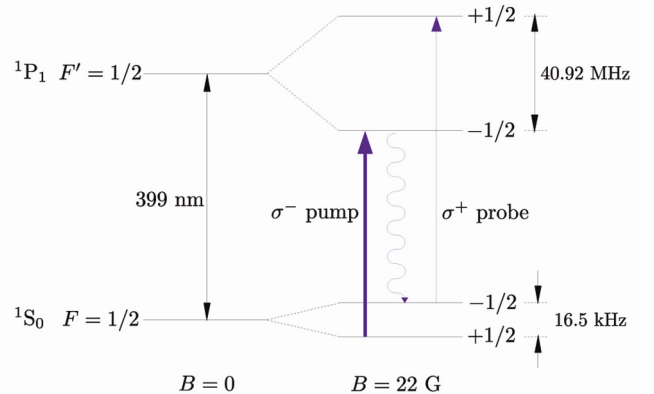


**Figure 2.** (Colour on-line). Splitting of the ground  $^1S_0$  level and the excited  $^1P_1$  level in  $^{171}\text{Yb}$  in the presence of a magnetic field  $B$ . Note that the splitting is opposite for the ground level because  $g_F$  is negative. The transitions coupled by the  $\sigma^-$  pump beam and the  $\sigma^+$  probe beam are shown. The wavy line represents spontaneous decay.

where  $\Omega'_R = \sqrt{\Omega_R^2 + \Delta^2}$  is the effective Rabi frequency. Since the atoms emanate from a thermal source, the beam consists of atoms with the following longitudinal velocity distribution<sup>8</sup>

$$f(v) = 2 \left( \frac{m}{2k_B T} \right)^2 v^3 \exp\left(-\frac{mv^2}{2k_B T}\right), \quad (4)$$

so that  $f(v)dv$  is the number of atoms with velocity between  $v$  and  $v + dv$ . The total probability  $P$  in an atomic beam is thus the probability for one velocity given in eq. (3) averaged over the velocity distribution given by eq. (4). Hence

$$P = \int_0^\infty pf(v)dv. \quad (5)$$

Since in the experiment we detect the population that has stayed in the  $m_F = -1/2$  sublevel, the fluorescence signal is proportional to  $(1 - P)$ . The calculated probability is compared to the observed signal below.

For the optical pumping to work effectively, the pump laser needs to be locked as close as possible to the  $m_F = +1/2 \rightarrow m_{F'} = -1/2$  transition in  $^{171}\text{Yb}$  (see Figure 2). But this is not as straightforward as it seems because of the presence of the overlapping peak from the even isotope  $^{170}\text{Yb}$ . This will affect the lock point significantly because the two peaks are partially resolved, as seen from the zero-field spectrum shown in Figure 3a. This problem can be solved using a magnetic field to shift the sublevels, and using circularly polarized light so that  $\Delta m$  selection rules imply that only a subset of transitions is allowed. But with  $\sigma^+$  polarized light, this still leads to an issue because the final spectrum has two peaks, as shown in the inset of Figure 3b. On the other hand, with  $\sigma^-$  polarized light, there is only one peak, as shown in Figure 3b. This is actually an unresolved peak containing both the  $+1/2 \rightarrow -1/2$  transition in  $^{171}\text{Yb}$  and the  $0 \rightarrow -1$  transition in  $^{170}\text{Yb}$ , but the presence of this additional transition is unimportant because optical pumping only requires the pump laser to be on the correct transition. This is one of the main reasons for choosing  $\sigma^-$  polarization for the pump beam.

The experimentally observed Ramsey pattern is shown in Figure 4b. To understand the lineshape, we have done a theoretical calculation of the expected signal, which is shown in Figure 4a. The theoretical calculation was done according to the procedure earlier in the text. The coil length  $\ell$  and the free evolution distance  $L$  are adjusted to get a good fit. The geometrical dimensions are  $\ell = 10$  mm and  $L = 440$  mm (see Figure 1), whereas the best fit is obtained with values of 40 mm and 400 mm. This increase in  $\ell$  (and corresponding decrease in  $L$ ) is reasonable because of the fringing fields from the coils extending beyond their physical edge, and the fact that their mean diameter is much larger than the size of

atomic beam. Changing the oven temperature [which determines the velocity distribution in eq. (4)] has negligible effect on the calculation, and it is left at 400°C.

As seen in the figure, the lineshapes for theory and experiment match quite well. The central fringe is located at 16.64 kHz corresponding to a magnetic field of 22.2 G, which is in good agreement with the value calculated from the coil dimensions. The linewidth  $\Delta\omega$  for the central fringe in both theory and experiment is about 350 Hz (0.47 G). If we roughly define SNR using the experimental uncertainty  $\delta\omega$  in determining the location of the central fringe as

$$\delta\omega = \frac{\Delta\omega}{\text{SNR}},$$

then SNR for the data shown is about 200. This is better than the SNR that we obtained using another technique for magnetometry called chopped NMOR<sup>4</sup>, which has also been proposed for use in precision measurements. The present technique has the additional advantage of measuring only the average field in the region between the oscillatory fields, and not being sensitive to field inhomogeneities in this region.

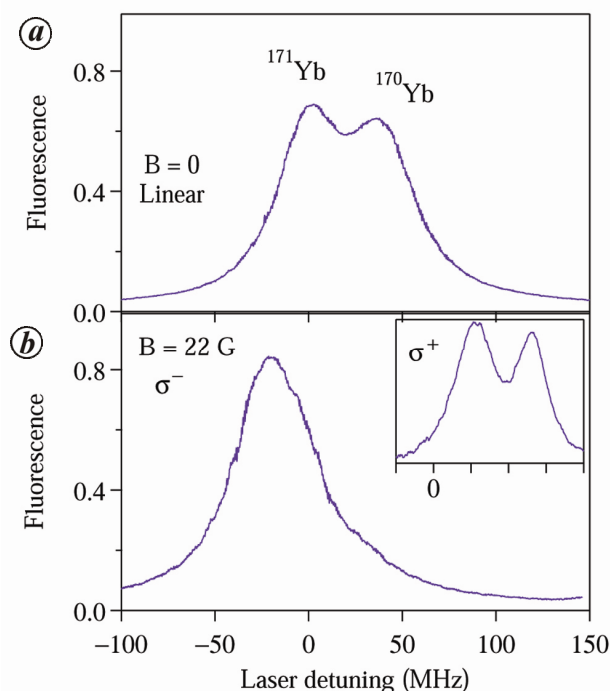


**Figure 3.** (Colour on-line). Scheme for locking the laser. **a**, Peaks corresponding to the  $^{171}\text{Yb}$  ( $F = 1/2 \rightarrow F' = 1/2$ ) transition and the  $^{170}\text{Yb}$  ( $F = 0 \rightarrow F' = 1$ ) transition are partially resolved in zero field, preventing proper locking of the laser. **b**, There is only a single peak in the presence of a magnetic field and when the laser beam has  $\sigma^-$  polarization, the peak is actually unresolved consisting of both the  $^{171}\text{Yb}$  ( $m_F = +1/2 \rightarrow m_{F'} = -1/2$ ) and the  $^{170}\text{Yb}$  ( $m_F = 0 \rightarrow m_{F'} = -1$ ) transitions, which are unimportant as explained in the text. (Inset) Choosing  $\sigma^+$  polarization also leads to two partially resolved peaks, corresponding to the  $^{171}\text{Yb}$  ( $m_F = -1/2 \rightarrow m_{F'} = +1/2$ ) and the  $^{170}\text{Yb}$  ( $m_F = 0 \rightarrow m_{F'} = +1$ ) transitions. All peaks are shifted from 0 because of the magnetic field.

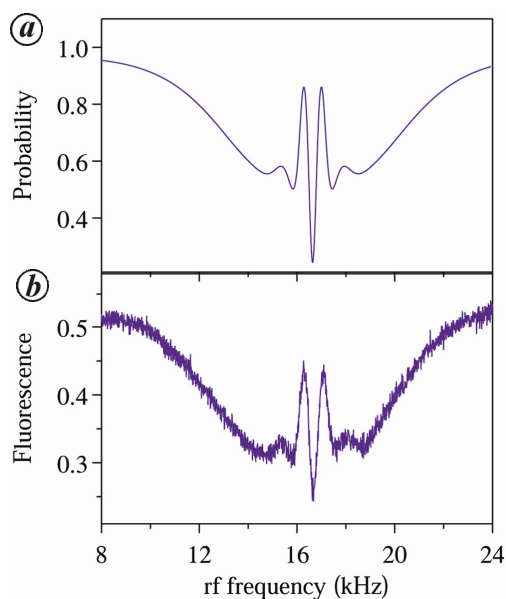


**Figure 4.** (Colour on-line). Theoretical and experimental Ramsey fringe spectra as a function of rf frequency. **a**, Calculated probability of atoms being in the  $m_F = -1/2$  sublevel, averaged over the thermal velocity distribution. **b**, Measured fluorescence signal from the  $\sigma^+$  probe beam, corresponding to population in the  $m_F = -1/2$  sublevel. The central fringe in both cases has a width of 350 Hz.

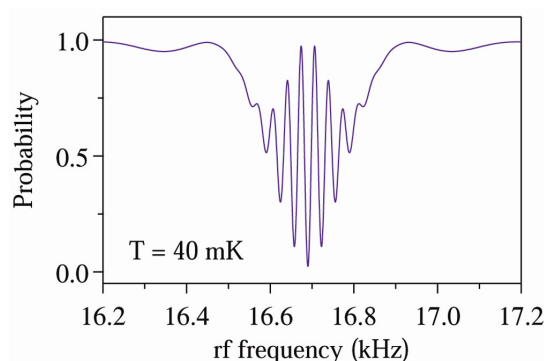


**Figure 5.** (Colour on-line). Calculated Ramsey pattern for a cold atomic beam with a longitudinal temperature of 40 mK. All parameters are the same as those used in Figure 4, except for the rf strength as discussed in the text. The scan range is only 1 kHz, and the central fringe has a width of 15 Hz.

Currently, the best sensitivity in magnetometry has been reported for a cell-based NMOR magnetometer, with a sensitivity of  $70 \text{ fT}/\sqrt{\text{Hz}}$  at  $7.6 \mu\text{T}$  being demonstrated<sup>9</sup>. Our beam experiment is expected to attain better sensitivity – but for a larger value of the field as demonstrated here, and as required for several applications such as EDM measurements – if we implement the technique with a cold atomic beam, of the kind demonstrated by us in earlier work, both using a 2D magneto-optic trap<sup>10</sup> and 1D molasses<sup>11</sup>. In the second experiment, the cold beam consisted of atoms travelling with a mean velocity of 15 m/s at a longitudinal temperature of 40 mK. To observe the likely improvement, we have repeated the calculation for this temperature. The values of  $B$ ,  $\ell$  and  $L$  are

left unchanged; only the rf strength is adjusted to provide a  $\pi/2$  pulse for atoms travelling at 15 m/s. The results are shown in Figure 5. Note that the scan range is only 1 kHz, which is 16 times smaller than for the previous one. The number of fringes has increased, and there is a dramatic decrease in linewidth of the central fringe from 350 to 15 Hz. This illustrates the advantage of using a cold beam for precision measurements.

In summary, we have demonstrated magnetometry using Ramsey's SOF technique in a thermal beam of Yb atoms emanating from an oven at  $400^\circ\text{C}$ . The experiment was done on the  $^1\text{S}_0 \rightarrow ^1\text{P}_1$  transition at 399 nm, and using the isotope  $^{171}\text{Yb}$  which has  $I = 1/2$ , and hence just two magnetic sublevels in the ground state. Using a quantization field of 22.2 G, we obtain a linewidth of 350 Hz at 16.64 kHz for the central fringe in the Ramsey pattern. The lineshape and linewidth agree with the theoretically calculated transition probability, after averaging over the thermal velocity distribution. The SNR is comparable to rival techniques of magnetometry, and we expect more than an order-of-magnitude increase in sensitivity when implemented with a cold beam.

- Schuh, B., Kanorsky, S. I., Weis, A. and Hänsch, T. W., Observation of Ramsey fringes in nonlinear Faraday rotation. *Opt. Commun.*, 1993, **100**, 451–455.
- Natarajan, V., Proposed search for an electric-dipole moment using laser-cooled  $^{171}\text{Yb}$  atoms. *Eur. Phys. J. D*, 2005, **32**, 33–38.
- Ramsey, N. F., A molecular beam resonance method with separated oscillating fields. *Phys. Rev.*, 1950, **78**, 695.
- Ravishankar, H., Chanu, S. R. and Natarajan, V., Chopped nonlinear magneto-optic rotation: a technique for precision measurements. *Europhys. Lett.*, 2011, **94**, 53002.
- Pustelny, S., Jackson Kimball, D. F., Rochester, S. M., Yashchuk, V. V. and Budker, D., Influence of magnetic field inhomogeneity on nonlinear magneto-optical resonances. *Phys. Rev. A*, 2006, **74**, 063406.
- Metcalf, H. J. and van der Straten, P., *Laser Cooling and Trapping*, 1999, Springer.
- Gossard, A. C., Jaccarino, V. and Wernick, J. H., Ytterbium NMR:  $^{171}\text{Yb}$  nuclear moment and Yb metal Knight shift. *Phys. Rev.*, 1964, **133**, A881–A884.
- Ramsey, N. F., *Molecular Beams*, Oxford University Press, Oxford, 1956.
- Lucivero, V. G., Anielski, P., Gawlik, W. and Mitchell, M. W., Shot-noise-limited magnetometer with sub-pico tesla sensitivity at room temperature. *Rev. Sci. Instrum.*, 2014, **85**, 113108.
- Rathod, K. D., Singh, A. K. and Natarajan, V., Continuous beam of laser-cooled Yb atoms. *Europhys. Lett.*, 2013, **102**, 43001.
- Rathod, K. D., Singh, P. and Natarajan, V., Cold beam of isotopically pure Yb atoms by deflection using 1D optical molasses. *Pramana*, 2014, **83**, 387–393.

**ACKNOWLEDGEMENTS.** This work was supported by the Department of Science and Technology, New Delhi, through the Swarnajayanti fellowship. We thank Sambit Pal for help with an initial version of this experiment, and for designing the audio amplifier. K.D.R. thanks the Council of Scientific and Industrial Research, New Delhi for financial support.

Received 17 March 2015; revised accepted 8 April 2015